Supplementary Information

Supplementary data - Materials and methods

Cell Culture

Rat renal fibroblasts (NRK-49F) were purchased from DSMZ (Germany collection of microorganisms and cell cultures, Braunschweig, Germany). NRK-49F cells were expanded and cultured according to manufacturer's instructions, using DMEM medium high glucose + 5% fetal calf serum (FCS) (Invitrogen, Paisley, Scotland) in 75 cm^2 flask in 5% CO_2 37°C incubator. Cells were starved with starving medium (RPMI 1640 + L-glutamine (Invitrogen, Paisley, Scotland)) when cells reached 70-80% confluence. Cells were stimulated by PDGF-BB (Sigma Aldrich, Deisenhofen, Germany) with concentration of 1, 10 and 50 ng/ml or by PDGF-DD (R&D Systems, Minneapolis, MN) with concentration of 10, 50 and 100 ng/ml. Then cells were collected 48 h after stimulation and subjected to various analyses.

Single-cell RNA sequencing

We reanalyzed the published data from Kramann et al. (*17*), which investigated $PDGFRb^+/CD45^+$ and $PDGFRb^+/CD45^-$ sorted cells from day 10 UUO kidneys of C57BL/6N mice. The read count of 51,810 genes was measured by using STAR (STAR_2.5.3a) (*38*) and HTSeq (version 0.9.1) (*39*) from the fastq file provided by GSE112033 with mouse primary assembly GRCm38. In order to remove low-quality cells and genes, we filtered out cells for which both library sizes and number of genes was lower than three median absolute deviations in log-space of all cells. In addition, we removed cells for which the read count of mitochondrial genes occupied more than 20% of the library size of the cell.

Inductively coupled plasma mass spectrometry

Elemental gadolinium quantification in kidneys was performed with inductively coupled plasma mass spectrometry (ICP-MS). Tissues (10-30 mg) were mineralized in digestion medium (1.5 ml HNO_3 65% + 1.5 ml H_2O_2 + 1 ml IS (Rhodium (1 µg/ml)) for 45 min at room temperature and heated to 210°C for 15 min. Gadolinium was measured by ELAN DRC II (Perkin Elmer Life and Analytical Sciences, Shelton, CT, USA). To make sure that the instrument was clean and optimized, spectral interferences were checked and reduced or eliminated before measurement. Rhodium (1 µg/ml) was used as internal standard. A standard curve was generated over the internal standard. Measurement results were compared to the standard curves and gadolinium concentration was calculated and normalized to the weight of kidney tissue used for the analyses.

Laser ablation inductively coupled plasma mass spectrometry

Kidney samples were cryo-cut into slices of 30 µm thickness with a cryomicrotome CM3050S (Leica Biosystems, Wetzlar, Germany) on -18°C cryo-chamber temperature and -16°C object temperature, thaw-mounted onto adhesive Starfrost® microscope slide (Knittel Glass, Braunschweig, Germany), dried and stored at room temperature. Tissue sections were photographed at 4x magnification with a light microscope IX81 (Olympus, Hamburg, Germany) to position the image dimensions. The distribution of gadolinium and other elements in sections of kidney tissues were systemically scanned (line by line) with a focused laser beam by LA-ICP-MS Xseries 2 (Thermo Fisher Scientific, Bremen, Germany) directly connected with a Nd:YAG laser ablation unit NWR260 (New Wave, Fremont, CA, USA). Matrix-matched tissue standards with well-defined concentrations of gadolinium were used as reference. Images were generated from LA-ICP-MS data using a Microsoft Excel 2007-based software tool with user-defined functions in Microsoft Excel VBA (termed ELAI) (*40*).

Supplementary data - Figures

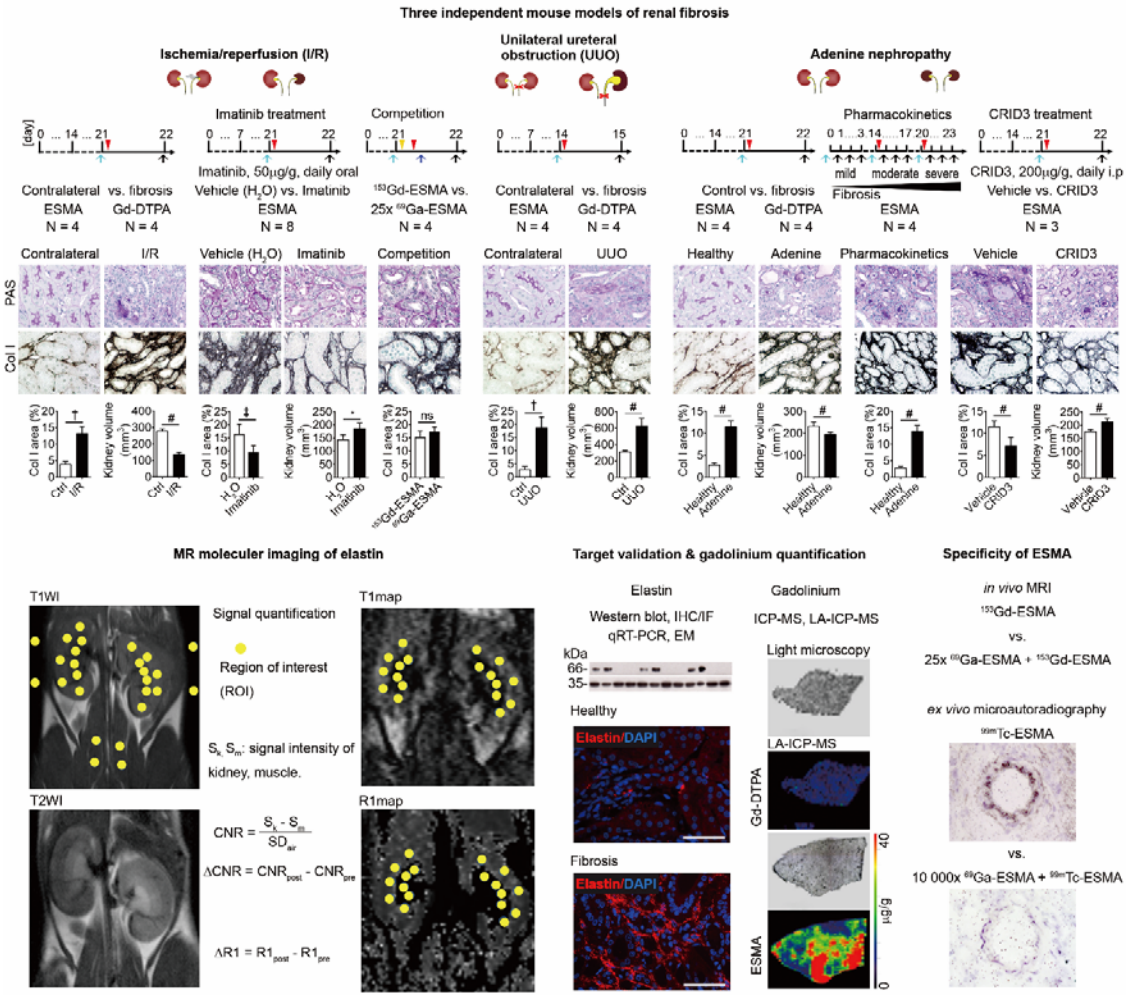

Fig. S1. Scheme of in vivo molecular MRI of renal fibrosis in three independent mouse models of renal fibrosis. Upper panel: experimental design and confirmation of renal fibrosis by PAS and collagen I staining. Red triangles represent injection of contrast agents, blue and black arrows show MRI scanning before and 24 h after injection, respectively. In the competition experiment an additional orange triangle shows injection of 25-fold dose of ^{69}Ga-ESMA and dark blue arrow shows MRI scanning 4 h after injection of 153Gd-ESMA. Collagen I positive area % and kidney volume were quantified. Lower left panel: methodology to quantify normalized MRI signal intensities and R1 echo times with $T1_W$I and T1 relaxometry measurement, respectively. Lower middle panel: ex vivo confirmation of elastin expression and Gd distribution. Lower right panel: proof of ESMA specificity by in vivo MRI and ex vivo microautoradiography competition experiments. PAS: Periodic acid-Schiff; IHC/IF: immunohistochemistry/fluorescence; EM: electron microscopy; LA-ICP-MS: laser ablation-inductively coupled plasma mass spectrometry. Scale bar: 50 µm. *P < 0.05, †P < 0.01, ‡P < 0.001, #P < 0.0001, ns: not significant, *t* test.

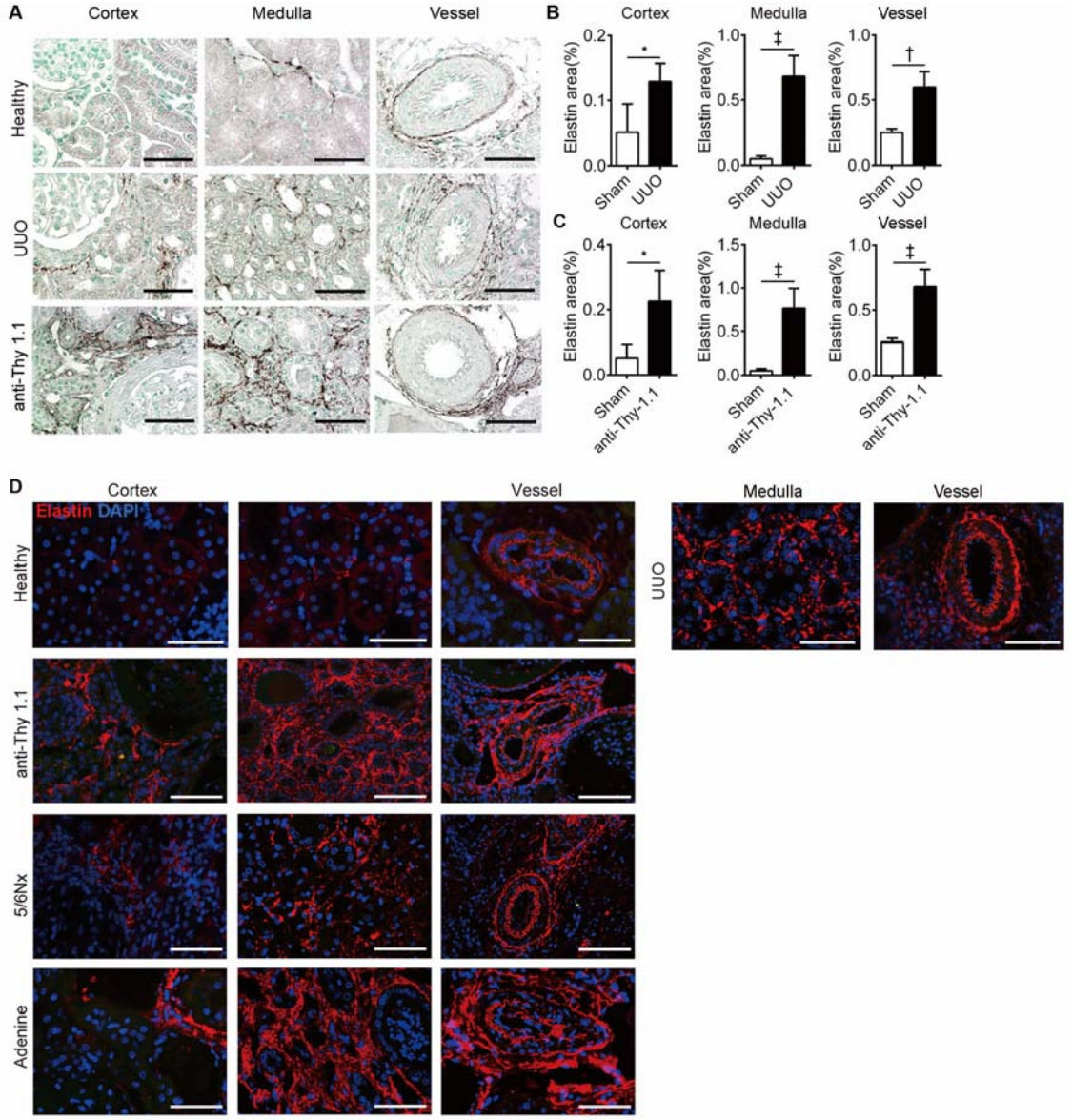

Fig. S2. Confirmation of increased elastin expression in renal fibrosis. (**A**) Immunohistochemical micrographs for elastin expression in UUO (n=4) and the anti-Thy 1.1 (n=4) rat model. (**B, C**) Quantification of elastin$^+$ area confirms increased elastin in renal fibrosis. (**D**) Representative images of immunofluorescent elastin stainings in anti-Thy 1.1, 5/6 nephrectomy (Nx), adenine as well as the UUO rat model. Scale bar, 50 µm.*P < 0.05, †P < 0.01, ‡P < 0.001, t test.

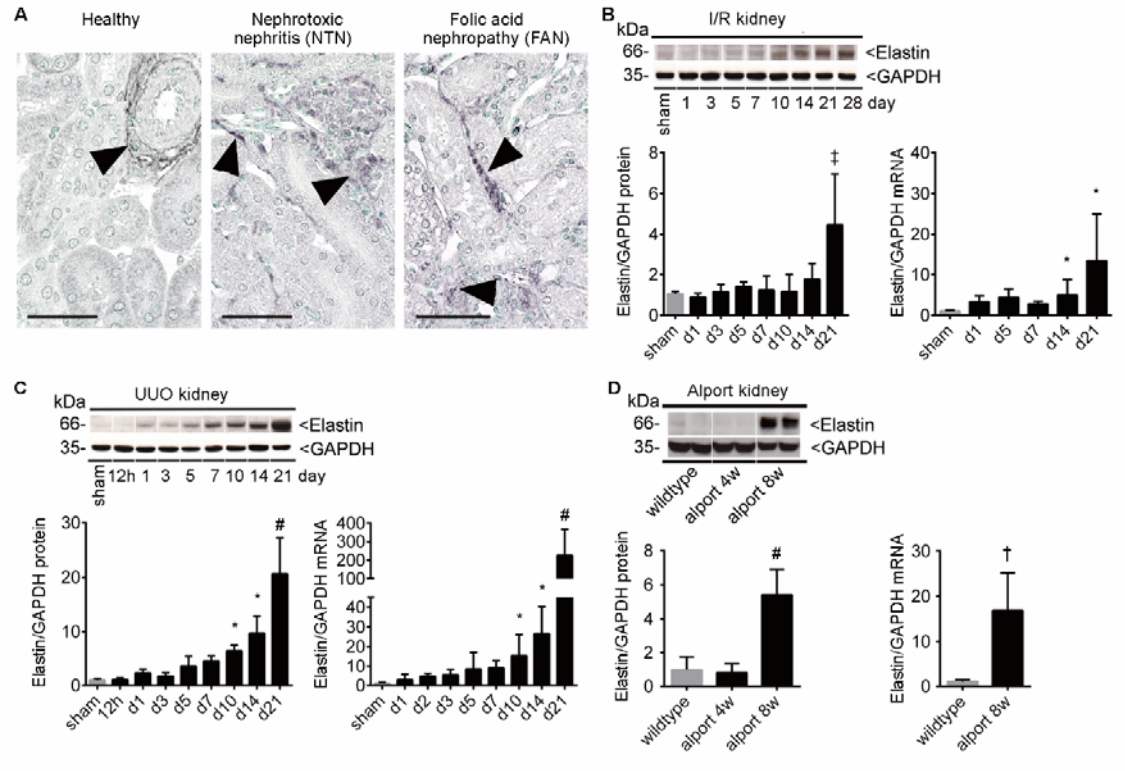

Fig. S3. Elastin expression in murine models of renal fibrosis. (**A**) Immunohistochemical staining shows interstitial elastin expression in mice with nephrotoxic serum nephritis (NTN day 14) and folic acid nephropathy (FA week 8) compared to healthy mice. (**B-D**) Western blot and qRT-PCR for elastin expression during progression of renal fibrosis in the (**B**) I/R mouse model (n=4 each time point), (**C**) UUO mouse model (n=5 each time point) and (**D**) Alport mouse model (n=4-5 each time point). Scale bar = 50 µm. **P* < 0.05, †*P* < 0.01, ‡*P* < 0.001, #*P* < 0.0001, one-way ANOVA test. *t* test for Alport kidney.

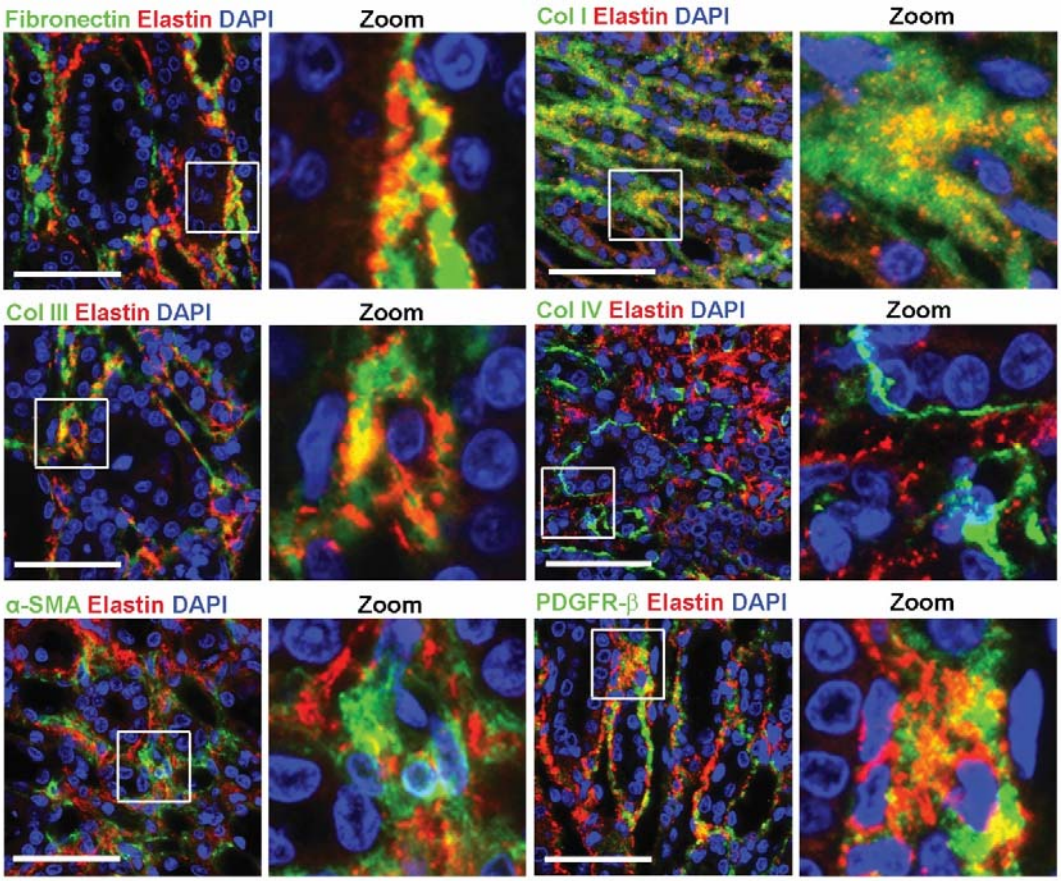

Fig. S4. Identification of interstitial (myo-)fibroblasts as elastin-producing cells in fibrotic kidneys. Immunofluorescent staining of elastin (red) and various specific markers (green). Elastin is co-localized with interstitial fibrotic tissue (fibronectin, collagen (Col) type I, Col III), and interstitial myofibroblasts (α-SMA and Platelet-derived growth factor receptor beta (PDGFR-β)), but did not co-localized with Col IV. Boxed areas are enlarged in the right panel. Scale bar: 50 μm.

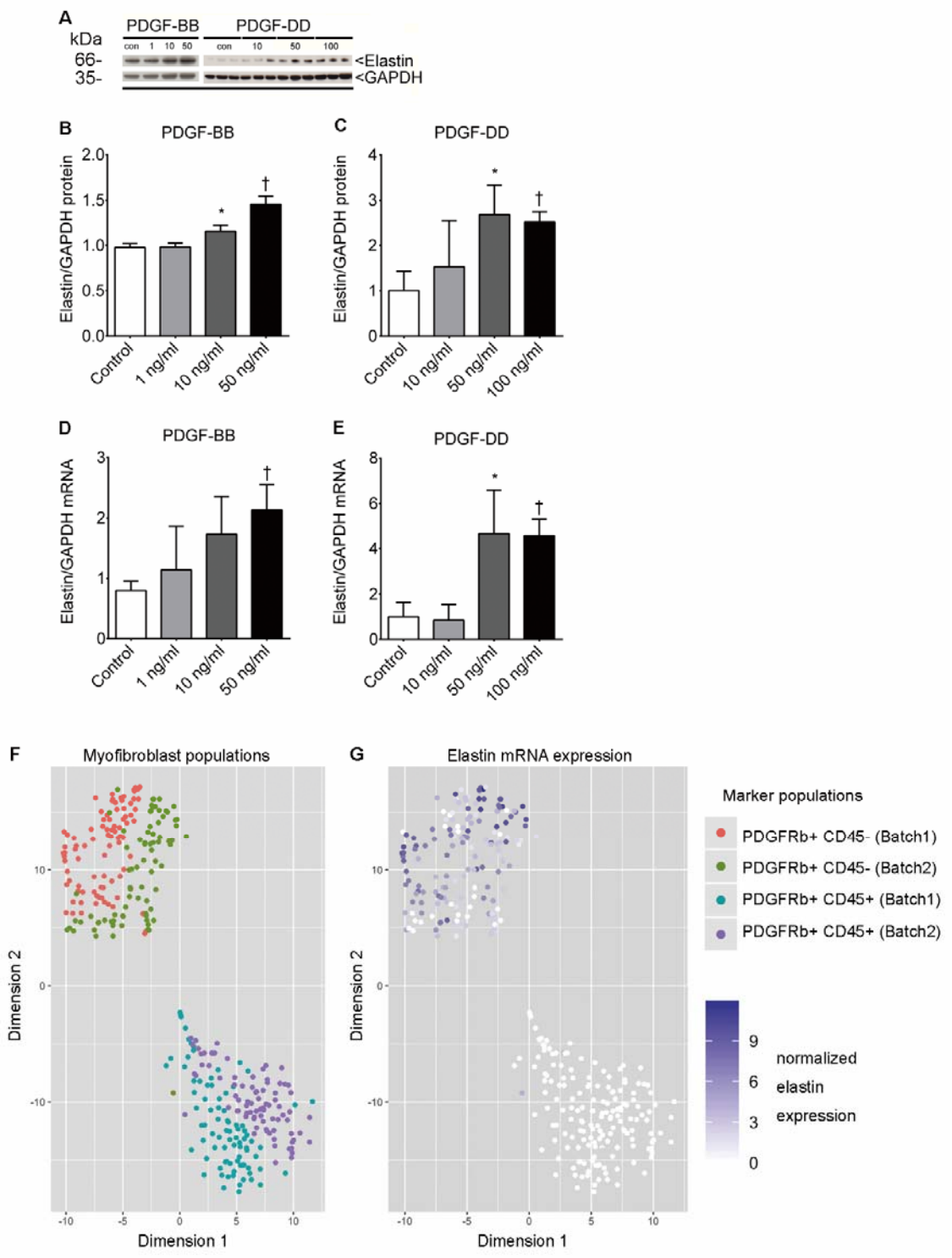

Fig. S5. Resident fibroblasts express elastin. (**A**) Representative Western blot and quantification of elastin protein as well as mRNA in NRK-49F fibroblast cell line after stimulation with PDGF-BB (**B, D**) and PDGF-DD (**C, E**). Single cell RNA sequencing data from UUO day 10 mice comparing resident myofibroblasts (PDGFR-β^{+}/CD45^{-}) and circulating myofibroblasts

(PDGFR-β^+/$CD45^+$) (**F, G**). Data are mean ± S.D and represent triplicate experiments. *$P < 0.05$, †$P < 0.01$, *t* test.

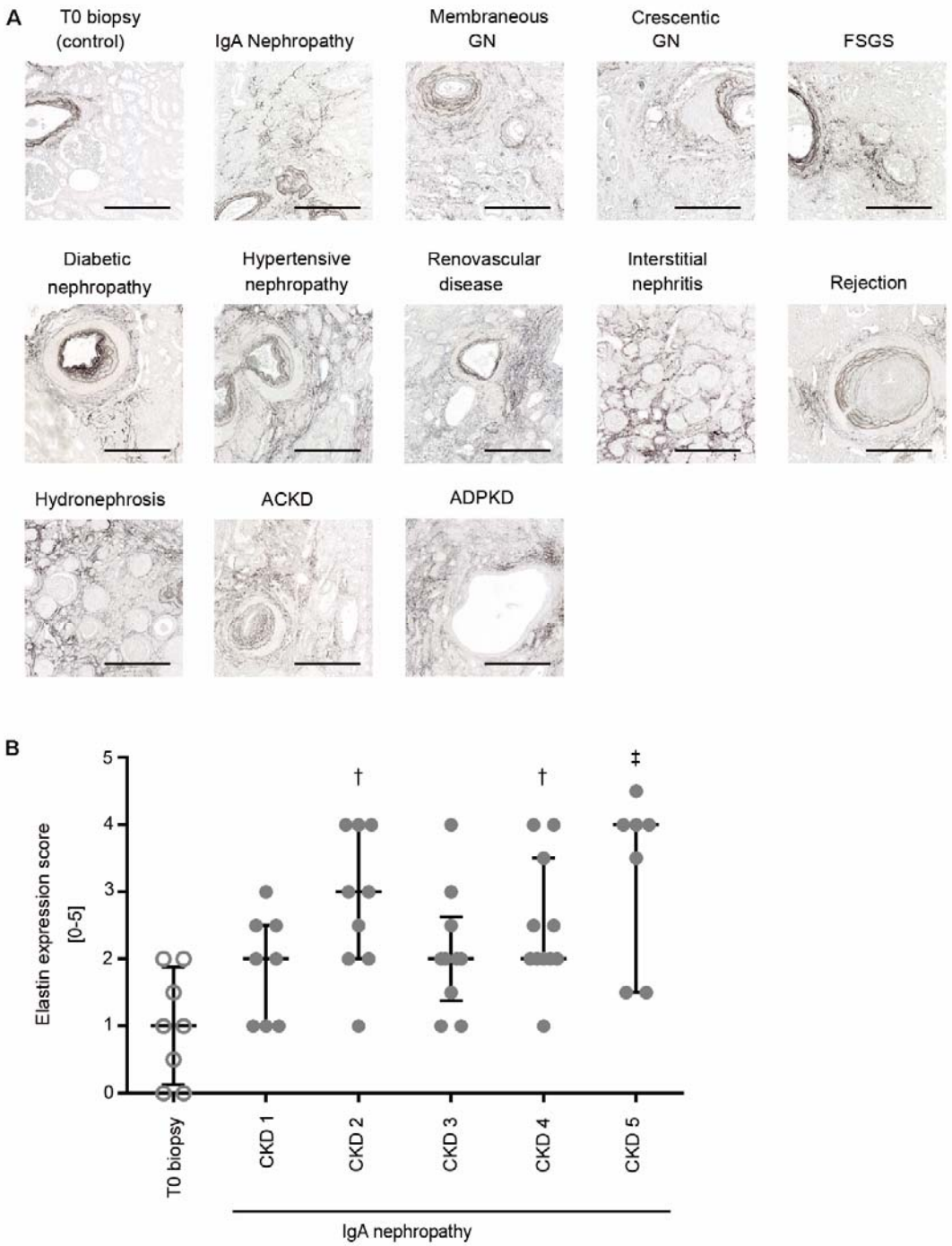

Fig. S6. Elastin expression in CKD patients. (**A**) Representative immunohistochemical micrographs from patients with various type of kidney disease. T0: protocol time zero biopsy of transplanted kidneys, Membranous GN: membranous glomerulonephritis, Crescentic GN: crescentic glomerulonephritis including Pauci-immune glomerulonephritis and Lupus nephritis, FSGS: focal segmental glomerulosclerosis, ACKD: acquired cystic kidney disease, ADPKD: autosomal dominant polycystic kidney disease. (**B**) Elastin expression is quantified in a cohort of patients with IgA nephropathy with different CKD stages (n=7-11). Scale bar = 250 µm. †$P < 0.01$, ‡$P < 0.001$, one way-ANOVA test with T0 biopsy.

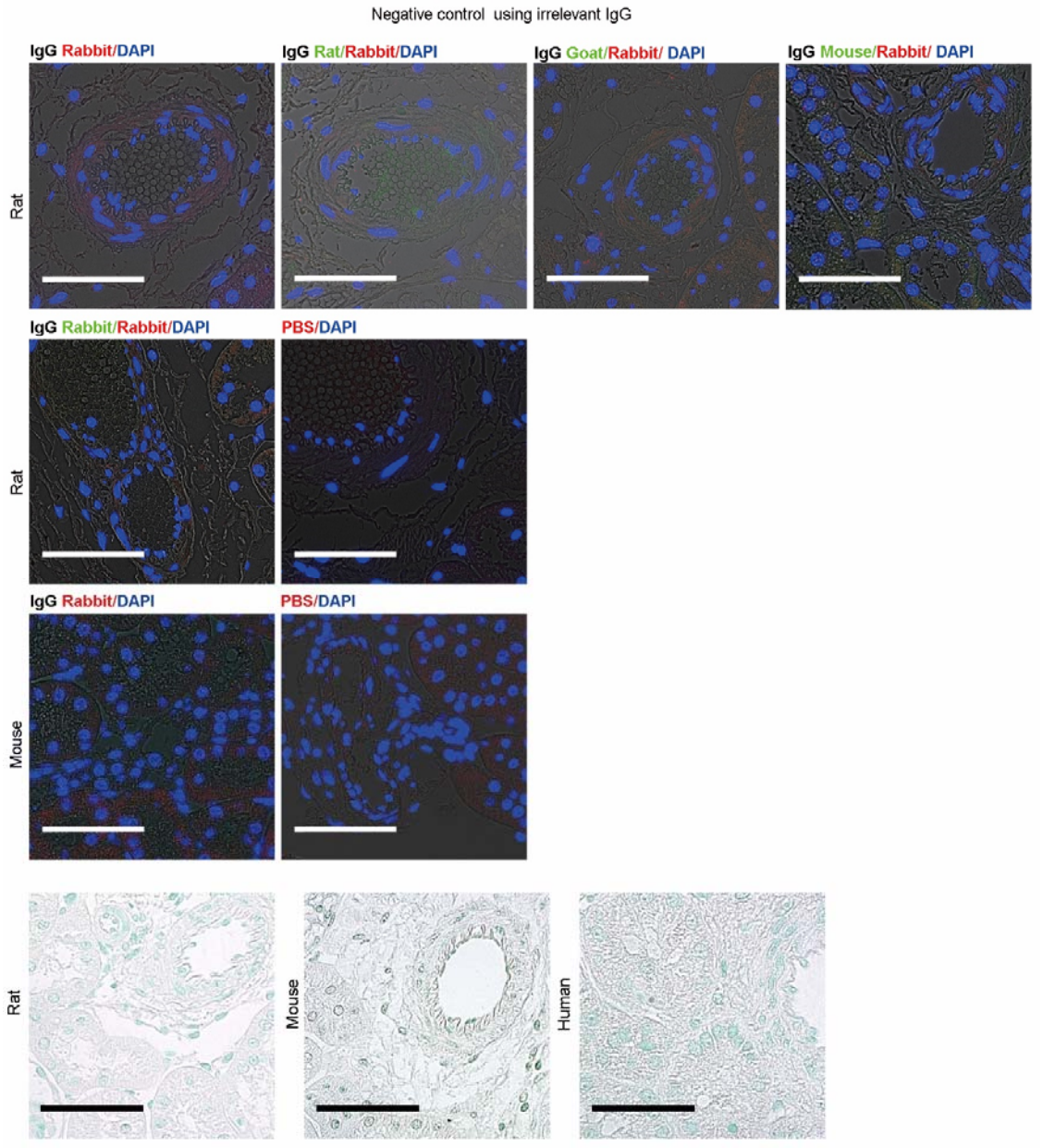

Fig. S7. Staining validation by means of non-specific secondary antibody and buffer control. Assessment of the specificity of the antibodies used for the histological evaluation with controls for non-specific binding of IgGs as secondary antibodies and PBS buffer as a control for tissue autofluorescence evaluation. Scale bar: 50 µm.

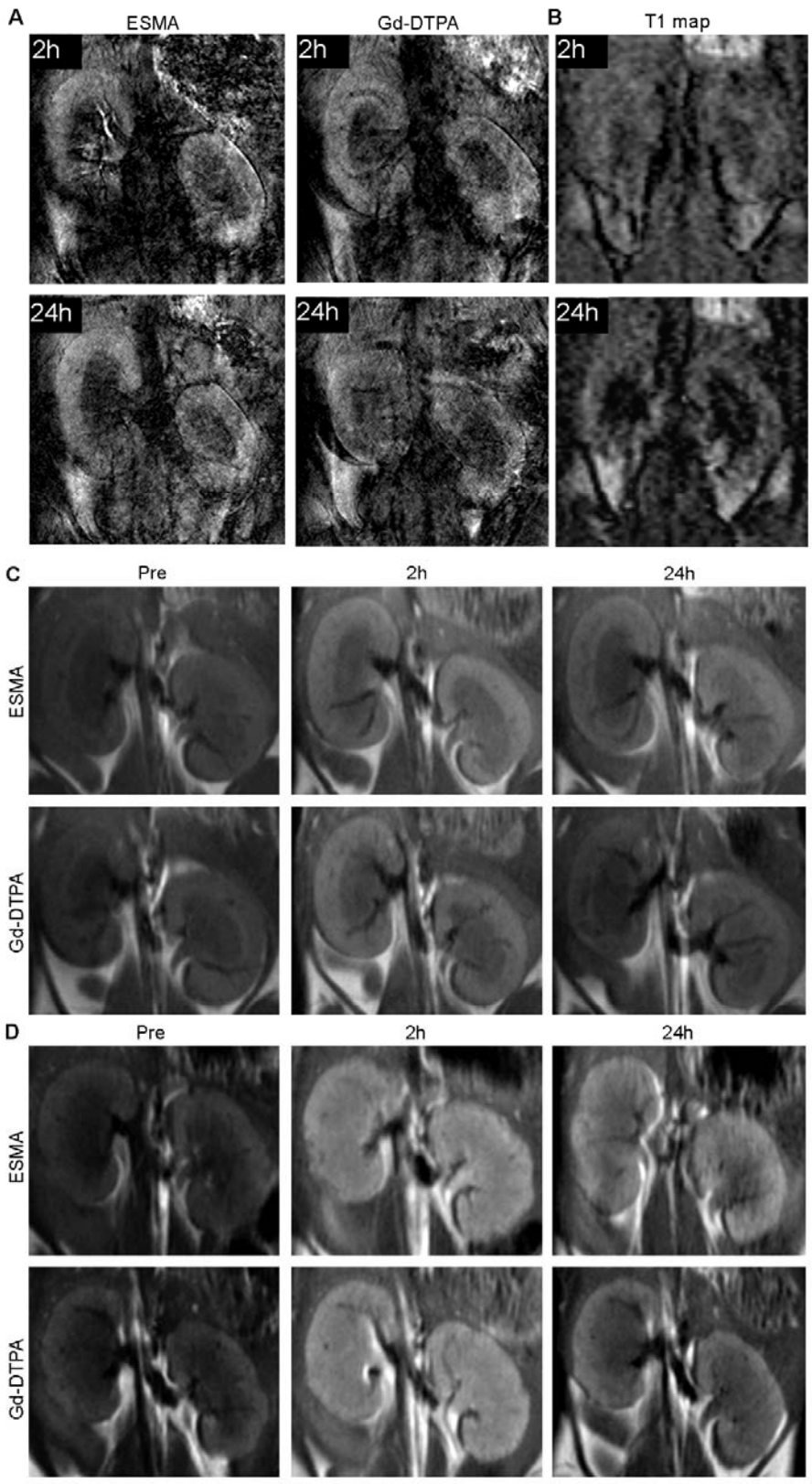
A
ESMA
Gd-DTPA
B
T1 map
2h
2h
2h
24h
24h
24h
C
Pre
2h
24h
ESMA
Gd-DTPA
D
Pre
2h
24h
ESMA
Gd-DTPA

Fig. S8. Feasibility assessment of different MRI sequences and measurement times. (**A**) Extreme motion artifacts are observed in T1-weighted inversion recovery turbo spin echo sequence. (**B**) T1 relaxometry measurement. (**C, D**) $T1_W$I images at different time points after i.v. injection identify 24 h as the preferred time point for ESMA-based non-invasive assessment of elastin content in both the I/R model (**C**) and adenine model (**D**).

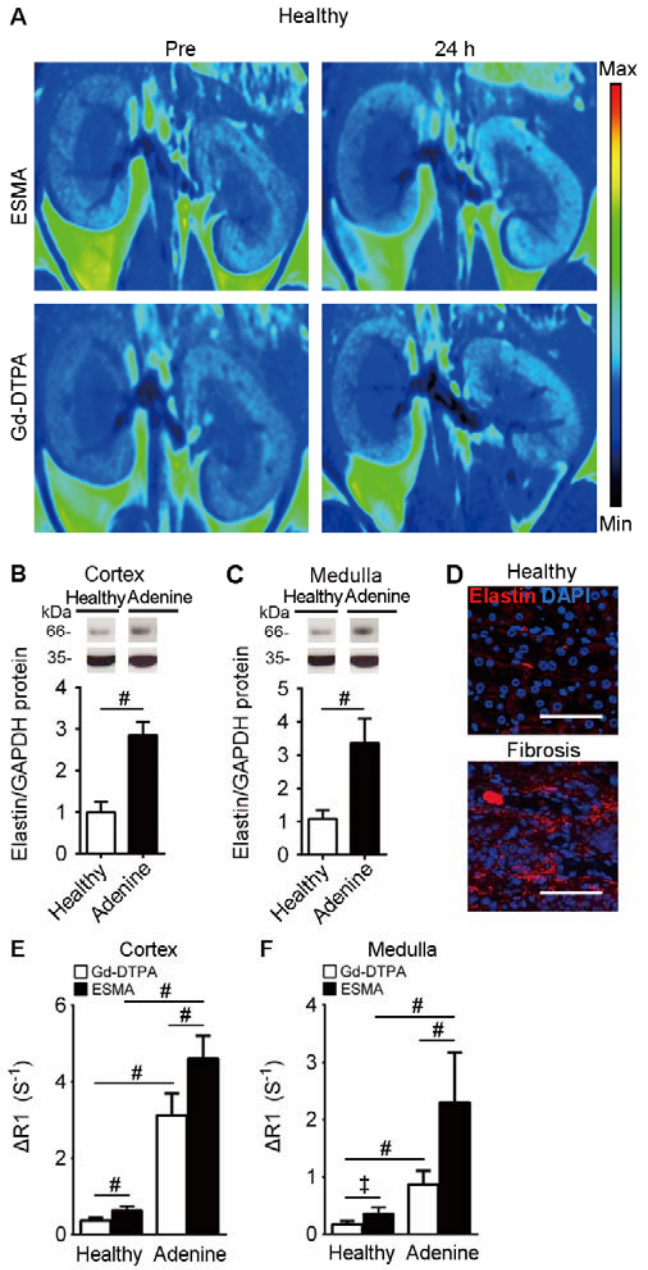

Fig. S9. Elastin imaging detects fibrosis in adenine nephropathy. (**A**) Color-coded images after injection with ESMA and Gd-DTPA in healthy kidneys. (**B, C**) Western blot and quantification of elastin in cortex and medulla in healthy (n=8) and fibrotic (n=8) kidneys. (**D**) Immunofluorescent microphotographs depict elastin in renal fibrosis. (**E, F**) ΔR1 changes in adenine model (n=4 for each group). ΔCNR: Δ contrast noise ratio. ‡$P < 0.001$, #$P < 0.0001$, *t* test.

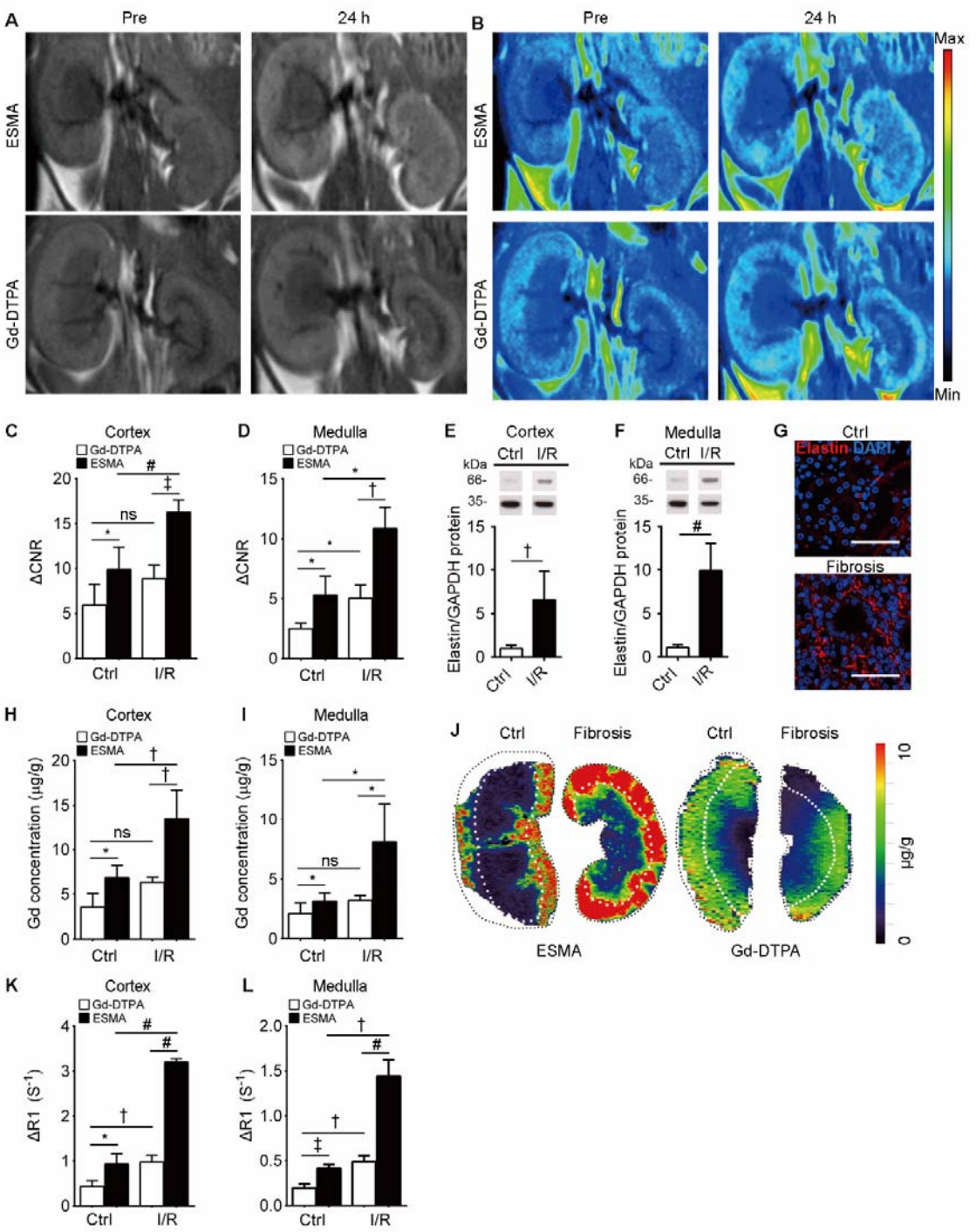

Fig. S10. Elastin imaging detects renal fibrosis in I/R. (**A**) Coronal T1wI and (**B**) pseudo color-coded images after injection of ESMA (n=4) and Gd-DTPA (n=4) in contralateral and I/R injured fibrotic kidneys. (**C, D**) Quantification of normalized MR signal intensities in cortex and medulla show differences between the ESMA and Gd-DTPA group in contralateral and fibrotic kidneys. (**E, F**) Western blot quantification of elastin in cortex and medulla as well as (**G**) immunofluorescent staining of elastin in renal fibrosis. (**H, I**) Gd quantification reflects the binding

of ESMA in fibrotic kidneys. (**J**) Gd distribution by LA-ICP-MS shows Gd accumulation in fibrotic kidneys in the ESMA group. (**K, L**) ΔR1 changes in I/R model. Ctrl: contralateral. Scale bar, 50 μm. ΔCNR: Δ contrast-to-noise ratio. $^{*}P < 0.05$, $^{\dagger}P < 0.01$, $^{\ddagger}P < 0.001$, $^{\#}P < 0.0001$, ns: not significant, *t* test.

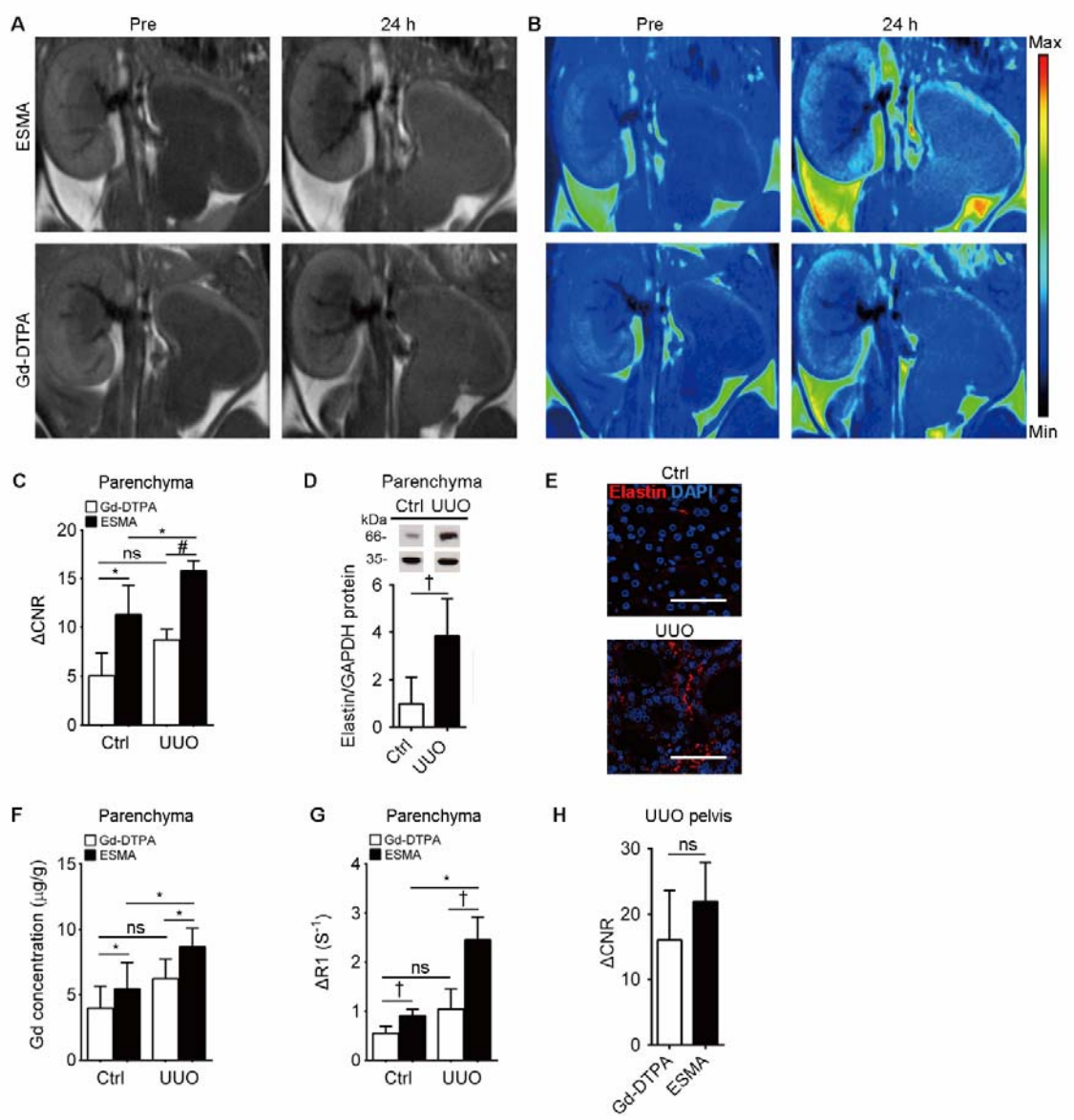

Fig. S11. Elastin imaging detects renal fibrosis in UUO. (**A**) Representative coronal T1WI and (**B**) pseudo color-coded images after injection with ESMA (n=4) and Gd-DTPA (n=4) in contralateral and UUO induced fibrotic kidneys. Extreme extension of left pelvis makes cortex and medulla indistinguishable. (**C**) Quantification of normalized MR signal intensities in parenchymal area (cortex plus medulla). (**D**) Representative Western blot and quantification of elastin in contralateral and fibrotic kidneys and (**E**) representative microphotographs of immunofluorescence of elastin in renal fibrosis. (**F**) Gd quantification reflects the binding of ESMA in fibrotic kidneys. (**G**) ΔR1 changes in UUO model. (**H**) ΔCNR shows no difference in pelvis between ESMA and Gd-DTPA. Ctrl: contralateral. Scale bar, 50 μm. ΔCNR, Δ contrast-to-noise ratio. $^{*}P < 0.05$, $^{\dagger}P < 0.01$, $^{\#}P < 0.0001$, ns: not significant, *t* test.

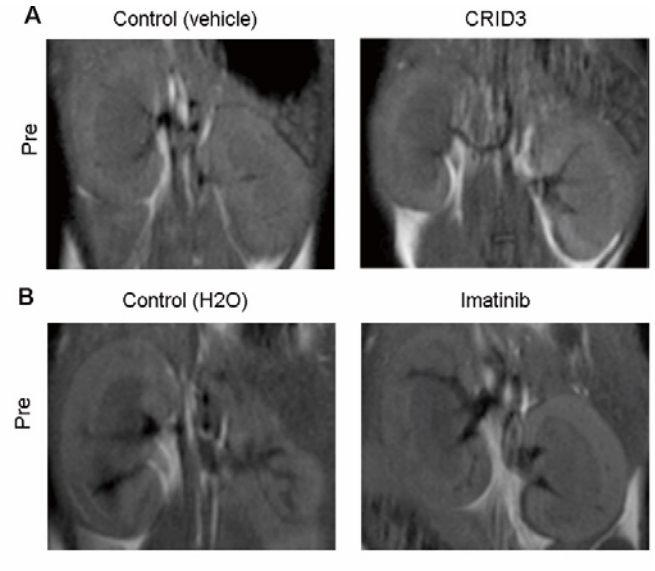

Fig. S12. Molecular MRI captures therapy effects in renal fibrosis.
(**A**) Representative MR images of adenine kidneys before ESMA injection and (**B**) I/R model on day 21 before contrast agent administration.

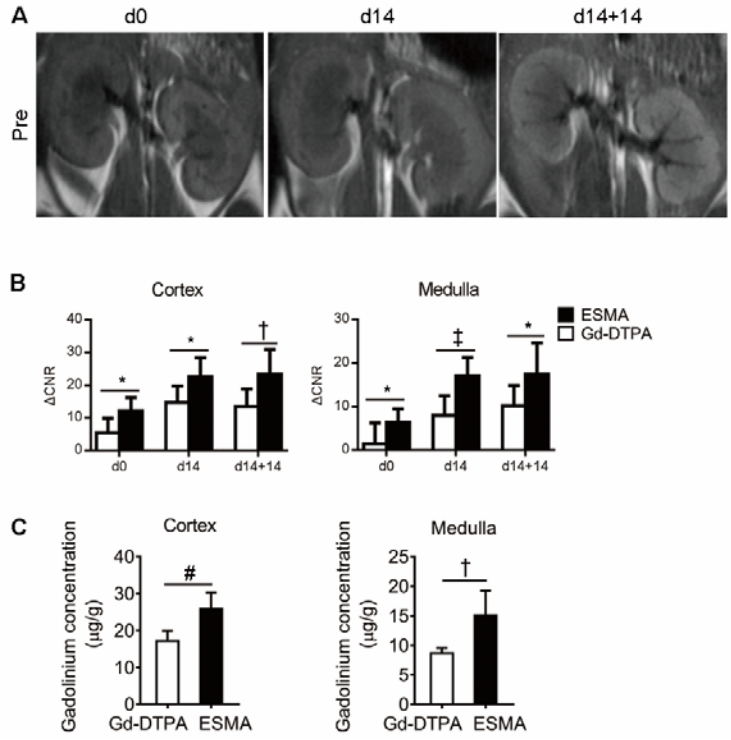

Fig. S13. Molecular MRI analysis of renal fibrosis vs. routine measurement of kidney function. (**A**) Representative MR images before injection of ESMA (n=4) and Gd-DTPA (n=4). (**B**) Quantification of normalized signal intensities of the cortex and medulla. (**C**) Gd quantification in both cortex and medulla of ESMA or Gd-DTPA injected kidneys. ΔCNR: Δ contrast-to-noise ratio. **P* < 0.05, †*P* < 0.01, ‡*P* < 0.001, #*P* < 0.0001, ns: not significant, *t* test.

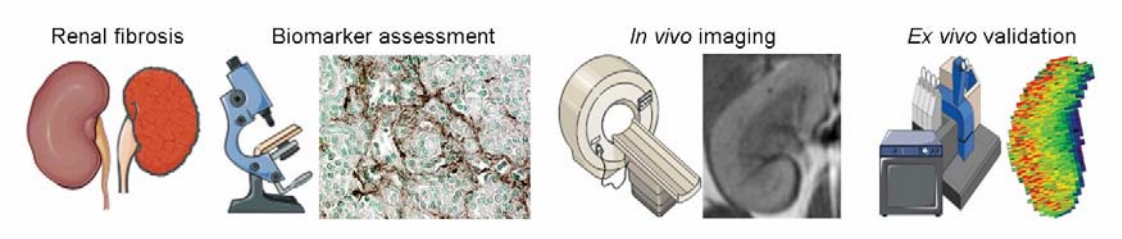

Fig. S14. Overall study and experimental design. (**A**) Schematic depiction of the experimental setup to analyze elastin expression and to assess its potential as an imaging biomarker for monitoring renal fibrosis.

Table S1. Collection of patient fibrotic kidney samples reflecting different kidney diseases. FFPE kidney samples from 89 patients were included in the study [9x time-zero biopsies (T0, non-fibrotic control), 5x tumor nephrectomies (non-tumor tissue, non-fibrotic control), 5 IgA nephropathy, 4x membranous nephropathy, 10x crescentic glomerulonephritis (GN, including 5x pauci-immune and 5x lupus nephritis), 5x focal segmental glomerulosclerosis (FSGS), 6 diabetic nephropathy (DN), 5x hypertensive nephropathy (HN), 3x renovascular disease, 7x interstitial nephritis, 14x transplant rejection (including acute and chronic, antibody and t-cell mediated), 6x hydronephrosis, 5x acquired cystic kidney disease (ACKD) and 5x autosomal dominant polycystic kidney disease (ADPKD)].

Disease	Sex	Age
T0 (non-fibrotic control)	M	55
T0 (non-fibrotic control)	M	66
T0 (non-fibrotic control)	M	70
T0 (non-fibrotic control)	M	55
T0 (non-fibrotic control)	M	43
T0 (non-fibrotic control)	F	70
T0 (non-fibrotic control)	M	67
T0 (non-fibrotic control)	M	53
T0 (non-fibrotic control)	M	67
Nephrectomy	M	77
Nephrectomy	M	54
Nephrectomy	F	3
Nephrectomy	F	47
Nephrectomy	n.a.	n.a.
IgA Nephropathy	M	50
IgA Nephropathy	M	35
IgA Nephropathy	M	27
IgA Nephropathy	M	44
IgA Nephropathy	M	36
Membranous GN	M	32
Membranous GN	M	25
Membranous GN	M	46
Membranous GN	M	39
Crescentic GN (Pauci immune)	F	65
Crescentic GN (Pauci immune)	F	74
Crescentic GN (Pauci immune)	F	45
Crescentic GN (Pauci immune)	F	78
Crescentic GN (Pauci immune)	F	59
Crescentic GN (Lupus)	F	41
Crescentic GN (Lupus)	M	55

Crescentic GN (Lupus)	F	19
Crescentic GN (Lupus)	F	68
Crescentic GN (Lupus)	F	40
FSGS	M	55
FSGS	M	36
FSGS	F	79
FSGS	M	47
FSGS	M	51
DN	M	46
DN	M	52
DN	F	46
DN	M	56
DN	M	37
DN	F	55
HN	M	51
HN	M	34
HN	M	56
HN	M	40
HN	M	71
Renovascular disease	M	47
Renovascular disease	M	70
Renovascular disease	M	72
Interstitial nephritis	M	68
Interstitial nephritis	M	89
Interstitial nephritis	M	63
Interstitial nephritis	F	46
Interstitial nephritis	F	43
Interstitial nephritis	M	5
Interstitial nephritis	F	16
Rejection	M	43
Rejection	F	58
Rejection	M	48
Rejection	F	60
Rejection	F	50
Rejection	M	55
Rejection	F	20
Rejection	F	73
Rejection	M	43
Rejection	M	28
Rejection	M	50
Rejection	M	47
Rejection	M	35
Rejection	M	66
Hydronephrosis	F	47

Hydronephrosis	F	47
Hydronephrosis	M	78
Hydronephrosis	M	56
Hydronephrosis	M	55
Hydronephrosis	M	25
ACKD	M	56
ACKD	F	53
ACKD	M	40
ACKD	M	46
ACKD	M	52
ADPKD	M	40
ADPKD	M	41
ADPKD	M	41
ADPKD	M	40
ADPKD	M	63

Table S2. IgA nephropathy patient cohort. Patients with IgA nephropathy and different stages of CKD (based on eGFR according to KDIGO). In total, 45 patients (8x CKD 1, 9x CKD 2, 10x CKD 3, 11x CKD 4, and 7x CKD 5) were included.

Disease	eGFR	CKD-Stage (KDIGO)
IgA nephropathy	117	1
IgA nephropathy	117	1
IgA nephropathy	102	1
IgA nephropathy	100	1
IgA nephropathy	113	1
IgA nephropathy	94	1
IgA nephropathy	95	1
IgA nephropathy	104	1
IgA nephropathy	60	2
IgA nephropathy	67	2
IgA nephropathy	85	2
IgA nephropathy	79	2
IgA nephropathy	78	2
IgA nephropathy	65	2
IgA nephropathy	86	2
IgA nephropathy	76	2
IgA nephropathy	62	2
IgA nephropathy	45	3
IgA nephropathy	41	3
IgA nephropathy	41	3
IgA nephropathy	32	3
IgA nephropathy	34	3
IgA nephropathy	n.a.	n.a.
IgA nephropathy	50	3
IgA nephropathy	42	3
IgA nephropathy	57	3
IgA nephropathy	44	3
IgA nephropathy	23	4
IgA nephropathy	24	4
IgA nephropathy	23	4
IgA nephropathy	15	4
IgA nephropathy	25	4
IgA nephropathy	15	4
IgA nephropathy	27	4
IgA nephropathy	29	4
IgA nephropathy	20	4
IgA nephropathy	28	4

IgA nephropathy	28	4
IgA nephropathy	14	5
IgA nephropathy	15	5
IgA nephropathy	9	5
IgA nephropathy	6	5
IgA nephropathy	9	5
IgA nephropathy	11	5
IgA nephropathy	11	5

Table S3. List of primers used for qRT-PCR. All sequences are provided in 5'→3' direction.

Gene	Forward primer	Reverse primer
Mouse		
Eln	TCTTGCTGATCCTCTTGCTCA	GGATAATAGACTCCACCGGGAA
Gapdh	GGCAAATTCAACGGCACAGT	AGATGGTGATGGGCTTCCC
Rat		
Eln	ATCGGAGGTCCAGGCATTG	ACCAGCACCAACCCCGTAT
Gapdh	ACAAGATGGTGAAGGTCGGTG	AGAAGGCAGCCCTGGTAACC
Human		
ELN	GCCATTCCTGGTGGAGTTCCTGGA	ACCGCACCTGCAGACACTCCTAAG
GAPDH	AGCCACATCGCTCAGACACC	GCGCCCAATACGACCAAA

ELN: elastin, *GAPDH*: glyceraldehyde-3-phosphate dehydrogenase.